NASA TN D-6707

OPTIMAL CRUISE TRAJECTORIES FOR SUPERSONIC AIRPLANES

by Fred Teren and Carl J. Daniele

Lewis Research Center

Cleveland, Ohio 44135

0133399

1. Report No. NASA TN D-6707	2. Government Accession No.	3. Recipient's Catalog No.
4. Title and Subtitle OPTIMAL CRUISE TRAJECTORIES FOR SUPERSONIC AIRPLANES		5. Report Date March 1972
		6. Performing Organization Code
7. Author(s) Fred Teren and Carl J. Daniele		8. Performing Organization Report No. E-6506
		10. Work Unit No. 110-06
9. Performing Organization Name and Address Lewis Research Center National Aeronautics and Space Administration Cleveland, Ohio 44135		11. Contract or Grant No.
		13. Type of Report and Period Covered Technical Note
12. Sponsoring Agency Name and Address National Aeronautics and Space Administration Washington, D.C. 20546		14. Sponsoring Agency Code

15. Supplementary Notes

16. Abstract

Equations are derived for maximizing range for specified initial and final values of mass and altitude. Constant-velocity flight is assumed, and normal acceleration is neglected. The problem is solved by using the maximum principle. Optimal trajectories are obtained and uniqueness is demonstrated. Results are obtained for a supersonic airplane. Curves are presented which can be used to obtain the optimal trajectory and maximum range for a range of initial and final mass and altitude. The optimal range is compared to the range obtained by using the standard cruise trajectory profile (consisting of a Breguet cruise plus maximum- and minimum-thrust connecting segments) and to the range obtained at constant-altitude cruise.

17. Key Words (Suggested by Author(s)) Optimal trajectories Cruise trajectories Airplane trajectories Breguet cruise	18. Distribution Statement Unclassified - unlimited		
19. Security Classif. (of this report) Unclassified	20. Security Classif. (of this page) Unclassified	21. No. of Pages 31	22. Price* $3.00

OPTIMAL CRUISE TRAJECTORIES FOR SUPERSONIC AIRPLANES

by Fred Teren and Carl J. Daniele

Lewis Research Center

SUMMARY

Equations are derived for maximizing range for specified initial and final values of mass and altitude. Constant-velocity flight is assumed, and normal acceleration is neglected.

The optimization problem is solved by using the maximum principle. The resulting optimal control histories are shown to consist at most of one maximum, one minimum, and one interior thrust arc. Optimal trajectories are obtained, and uniqueness is demonstrated. Results are obtained for a supersonic airplane. Curves are presented which can be used to obtain the optimal trajectory and maximum range for a range of initial and final mass and altitude. In addition, the optimal range is compared to the range obtained by using the standard cruise trajectory profile (consisting of a Breguet cruise plus maximum- and minimum-thrust connecting segments) and to the range at constant-altitude cruise. The difference between optimal and standard trajectory range is shown to be small.

INTRODUCTION

The optimization of airplane trajectories is generally considered as three separate optimization problems - takeoff and climb, cruise, and descent and landing. The optimal climb problem has been treated in the literature by using the energy-state approximation (ref. 1), as well as by treating a more precise formulation of the system equations with the attendant complexities (ref. 2). The descent phase is generally highly constrained, and therefore not subject to mathematical optimization. The importance of optimizing the cruise trajectory (maximizing cruise range) is obvious. Yet, this phase has received little attention in the literature. The reason for the lack of attention is that the approximations generally made in considering the cruise trajectory optimization reduce the solution to a nearly universal equation for all airplanes, the so-called Breguet range

equation. Furthermore, the Breguet cruise seems intuitively to be difficult to improve on, since the associated approximations seem to be quite reasonable.

The Breguet range equation is derived by assuming steady flight. All accelerations are assumed to be zero, and the climb rate is also neglected. Therefore, altitude becomes a control variable for the problem, and the Breguet range equation results. In the present study, the cruise trajectory model is made more realistic by including the altitude as a state variable. With this formulation, the cruise trajectory is defined as the portion of the flight at cruise velocity, with specified initial and final altitudes corresponding to the end of climb and the beginning of descent. The optimization problem is formulated by using the maximum principle (ref. 3). Costate equations are derived and are used to determine the optimum thrust level as a function of the state variables.

The procedure for obtaining optimal trajectories is illustrated for a supersonic airplane. A set of curves is presented from which maximum range can be determined for any values of initial and final mass and altitude. Comparisons are also made between the optimal range and the range obtained by using two suboptimal cruise trajectory profiles.

CRUISE RANGE OPTIMIZATION

Equations of Motion

It is desired to maximize range for an airplane with fixed initial and final mass. The velocity is assumed to be constant, and the initial and final altitudes are specified. The flight time is free. The equations of motion are

$$\dot{v} = \frac{1}{m} (T - D - mg \sin \gamma) \tag{1a}$$

$$\dot{\gamma} = \frac{1}{mv} (L - mg \cos \gamma) \tag{1b}$$

$$\dot{h} = v \sin \gamma \tag{1c}$$

$$\dot{m} = - \frac{T}{g} S \tag{1d}$$

All symbols are defined in the appendix; some of the variables are illustrated in figure 1. The thrust is assumed to be parallel to the airplane longitudinal axis, and the angle of attack is neglected. The specific fuel consumption S is a function of thrust and altitude.

2

Equations (1) apply for planar flight with a constant gravity field (that is, a flat Earth is assumed). The range is given by

$$R = \int_{t_0}^{t_f} v \cos \gamma \, dt \qquad (2)$$

Breguet Cruise

The Breguet equation has generally been used to calculate airplane cruise range. For completeness and for comparative purposes, the Breguet equation is derived in this section. The following assumptions are made:

(1) The normal acceleration $v\dot{\gamma}$ is negligible. This does not mean that γ is constant, only that the acceleration required to change γ is negligibly small.

(2) The vertical velocity $\dot{h}$ is negligible. Here again, h is not necessarily constant. Neglecting $\dot{h}$ requires setting $\sin \gamma = 0$ and $\cos \gamma = 1$ in equation (1). Furthermore, this assumption makes h a control variable.

Using these assumptions, along with constant velocity, gives for equations (1a) and (1b)

$$T = D \qquad (3a)$$

$$L = mg \qquad (3b)$$

and the range becomes

$$R = \int_{t_0}^{t_f} v \, dt = - \int_{m_0}^{m_f} \frac{vg \, dm}{TS}$$

This equation can be rewritten by using equation (3) as

$$R = - \int_{m_0}^{m_f} v \left(\frac{L}{DS}\right) \frac{dm}{m} \qquad (4)$$

which is the Breguet range equation. Maximum range for the Breguet cruise is obtained by maximizing, at each flight time (or mass), the value of L/DS. The maximization may be performed independently at each point along the trajectory since altitude is assumed to be a control variable and may be changed discontinuously if required.

At this point, it is useful to describe the airplane and atmospheric characteristics in more detail. The following assumptions are made:

(1) A parabolic drag polar is assumed; that is,

$$C_D = C_{D,0} + K C_L^2$$

where $C_{D,0}$ and K are constants, independent of altitude. The lift and drag are given by

$$L = C_L QA \qquad (5a)$$

$$D = C_D QA \qquad (5b)$$

where A is the reference area and Q is the dynamic pressure, defined by

$$Q = \frac{1}{2} \rho v^2 \qquad (6)$$

(2) An isothermal atmosphere is assumed; that is,

$$\rho = \rho_0 e^{-\beta h} \qquad (7)$$

This also implies that speed of sound is constant. Hence, Mach number remains constant during a constant-velocity cruise.

(3) The airplane specific fuel consumption is a function (for constant-velocity flight) only of the thrust coefficient C_F, where

$$C_F = \frac{T}{QA} \qquad (8)$$

In addition, C_F has upper and lower limits, $C_{F,u}$ and $C_{F,\ell}$, which are independent of altitude.

With these assumptions, the operating conditions for maximizing Breguet cruise range can be determined more explicitly:

$$\frac{L}{DS} = \frac{C_L QA}{C_D QAS} = \frac{C_L}{C_D S}$$

Equations (3a), (5b), and (8) can be combined to give $C_D = C_F$. Also, C_L can be expressed in terms of C_F as follows:

$$C_L = \sqrt{\frac{C_D - C_{D,0}}{K}} = \sqrt{\frac{C_F - C_{D,0}}{K}} \tag{9}$$

Therefore,

$$\frac{L}{DS} = \frac{1}{C_F S} \sqrt{\frac{C_F - C_{D,0}}{K}}$$

and the optimum C_F can be obtained by differentiating L/DS with respect to C_F (with $S = S(C_F)$) and setting it equal to zero. This results in the following equation, which can be solved for the optimum value of C_F:

$$\frac{C_F S}{2} - (C_F - C_{D,0})\left(S + C_F \frac{dS}{dC_F}\right) = 0 \tag{10}$$

It should be noted that the optimum value of C_F is independent of mass, and hence constant for the entire cruise trajectory. Also, from equation (9), C_L is constant; thus, it follows that L/D is also constant. In addition, since $C_L = L/QA = mg/QA$, $m/Q = AC_L/g = $ constant. Thus, Q must decrease (altitude increases) as mass decreases. The Breguet cruise range can be obtained by integration of equation (4) and using the fact that L/D is constant:

$$R = v\left(\frac{L}{DS}\right)_{max} \log\left(\frac{m_0}{m_f}\right) \tag{11}$$

Inclusion of Altitude Effect

In the derivation of the Breguet range equation, altitude was assumed to be a control variable and was allowed to change discontinuously if required. At this point, the problem will be stated more realistically by including altitude as a state variable. The state equations (1) may be rewritten by using equations (5) to (8) as

$$\dot{v} = \frac{QA}{m}\left(C_F - C_{D,0} - KC_L^2 - \frac{mg}{AQ}\sin\gamma\right) \tag{12a}$$

$$\dot{\gamma} = \frac{1}{mv}(C_L QA - mg\cos\gamma) \tag{12b}$$

$$\dot{Q} = -\beta Qv\sin\gamma + \frac{2Q^2 A}{mv}\left(C_F - C_{D,0} - KC_L^2 - \frac{mg}{QA}\sin\gamma\right) \tag{12c}$$

$$\dot{m} = -\frac{AQ}{g}C_F S(C_F) \tag{12d}$$

where the state variable h has been replaced by the equivalent state variable Q.

In order to simplify the problem, it will be assumed here (as it was in the derivation of the Breguet range equation) that normal acceleration is negligible, cruise velocity is constant, and γ is small (i.e., $\cos\gamma \approx 1$). However, the state variables Q and m will be retained. Setting equations (12a) and (12b) equal to zero, solving for $\sin\gamma$, and using this result in equation (12c) yield

$$\dot{Q} = -\frac{\beta Q^2 vA}{mg}\left(C_F - C_{D,0} - \frac{Kg^2 m^2}{A^2 Q^2}\right) \tag{13}$$

The optimization problem can now be stated as

$$\text{maximize}\int_{t_0}^{t_f} v\,dt \tag{14}$$

subject to the differential constraints

$$\dot{Q} = -\frac{\beta Q^2 vA}{mg}\left(C_F - C_{D,0} - \frac{Kg^2 m^2}{A^2 Q^2}\right) \tag{15a}$$

$$\dot{m} = -\frac{AQ}{g}C_F S \tag{15b}$$

an inequality constraint on the control C_F

$$C_{F,\ell} \leq C_F \leq C_{F,u}$$

and boundary conditions on Q and m. The problem is formulated by using the Pontryagin maximum principle in minimum form (ref. 3). The variational Hamiltonian can be written as

$$H = -v - \lambda_1 \frac{\beta Q^2 vA}{mg} \left(C_F - C_{D,0} - \frac{Kg^2 m^2}{A^2 Q^2} \right) - \lambda_2 \frac{AQ}{g} C_F S + \mu(C_F - C_{F,u})(C_F - C_{F,l}) \quad (16)$$

The costate equations are

$$\dot{\lambda}_1 = 2\lambda_1 \frac{\beta Q vA}{mg} (C_F - C_{D,0}) + \frac{\lambda_2}{g} AC_F S \quad (17a)$$

$$\lambda_2 = -\frac{\lambda_1 \beta Q^2 vA}{gm^2} \left(C_F - C_{D,0} + \frac{Kg^2 m^2}{A^2 Q^2} \right) \quad (17b)$$

The optimal C_F is obtained from

$$\frac{\partial H}{\partial C_F} = -\lambda_1 \frac{\beta Q^2 vA}{mg} - \lambda_2 \frac{AQ}{g} \frac{d}{dC_F} (SC_F) + \mu(2C_F - C_{F,u} - C_{F,l}) = 0 \quad (18)$$

and subject to

$$\frac{\partial^2 H}{\partial C_F^2} = -\frac{\lambda_2}{g} AQ \frac{d^2}{dC_F^2} (SC_F) + 2\mu \geq 0 \quad (19a)$$

and

$$\mu = 0 \quad (19b)$$

on interior arcs (i.e., $C_{F,l} < C_F < C_{F,u}$). The optimal thrust coefficient history may consist of maximum, minimum, and interior arcs. It is instructive to determine the variation of C_F on optimal interior arcs. It will be shown that an optimal interior arc is uniquely determined by initial values of C_L and C_F. On interior arcs, equations (18) and (19b) give

$$\frac{-\lambda_1 \beta Q v}{m} - \lambda_2 \frac{d}{dC_F} (SC_F) = 0 \qquad (20a)$$

For notational simplicity, let $a(C_F) = C_F S(C_F)$ and let $'$ denote differentiation with respect to C_F. Then equation (20a) may be written

$$\frac{a'}{\beta v} = -\frac{\lambda_1 Q}{\lambda_2 m} \qquad (20b)$$

Differentiation of equation (20b) with respect to time gives

$$\frac{a''}{\beta v} \dot{C}_F = -\frac{d}{dt}\left(\frac{\lambda_1 Q}{\lambda_2 m}\right) = -\frac{Q}{\lambda_2 m}\left[2\lambda_1 \frac{\beta Q v A}{mg} (C_F - C_{D,0}) + \frac{\lambda_2}{g} Aa\right]$$

$$+ \frac{\lambda_1 \beta A}{\lambda_2 m^2 g} Q^2 v \left(C_F - C_{D,0} - \frac{Kg^2 m^2}{A^2 Q^2}\right) - \frac{\lambda_1 Q^2 Aa}{\lambda_2 m^2 g} - \frac{\lambda_1^2 Q^3 \beta v A}{\lambda_2^2 m^3 g}\left(C_F - C_{D,0} + \frac{Km^2 g^2}{A^2 Q^2}\right)$$

Substituting for λ_1 / λ_2 from equation (20b) results in

$$\frac{a'' \dot{C}_F}{\beta v} = -\frac{Q}{mg} \frac{a' A}{\beta v} (a' - \beta v)\left(C_F - C_{D,0} + \frac{Km^2 g^2}{A^2 Q^2} - \frac{a}{a'}\right)$$

or, since $L = C_L Q A = mg$,

$$\dot{C}_F = \frac{a'}{a'' C_L} (\beta v - a')\left(C_F - C_{D,0} + KC_L^2 - \frac{a}{a'}\right) \qquad (21)$$

Thus, the rate of change of C_F on an interior arc is uniquely determined by the values of C_L and C_F (for given values of the airplane parameters). The rate of change of C_L on an interior arc can also be obtained by differentiation:

$$\dot{C}_L = \frac{d}{dt}\left(\frac{mg}{QA}\right) = -a + \beta v\left(C_F - C_{D,0} - KC_L^2\right) = \beta v\left(C_F - C_{D,0} - KC_L^2 - \frac{a}{\beta v}\right) \qquad (22)$$

so that the rate of change of C_L is also determined by the instantaneous values of C_F and C_L. A constant control arc (C_F constant) can exist only if C_L is also constant.

8

Thus,

$$C_F - C_{D,0} + KC_L^2 - \frac{a}{a'} = 0 \tag{23a}$$

and

$$C_F - C_{D,0} - KC_L^2 - \frac{a}{\beta v} = 0 \tag{23b}$$

must be satisfied simultaneously. The value of C_F on this arc is determined by solving

$$C_F = C_{D,0} + \frac{a}{2a'} + \frac{a}{2\beta v} \tag{24a}$$

The value of C_L can then be determined from equation (23b) as

$$C_L = \sqrt{\frac{C_F - C_{D,0} - \frac{a}{\beta v}}{K}} \tag{24b}$$

It is interesting to compare the constant control arc given by equation (24) with the Breguet cruise equations (9) and (10). If equation (10) is rewritten in terms of a, the result is

$$C_F = C_{D,0} + \frac{a}{2a'} \tag{25}$$

The similarity of equations (24) and (25) is evident. In fact, equation (24a) represents a modified Breguet cruise - modified by the additional thrust required to change altitude.

Construction of C_F - C_L Diagram

Because of the nonlinearity of the variational equations required for maximizing range, the optimal trajectories are very difficult to obtain by conventional methods (e.g., solution of the two-point boundary value problem). It was found that the important features of the optimal trajectories could be conveniently displayed on a graph of lift coefficient as a function of thrust coefficient. From these features, an approximate (but

9

quite accurate) procedure was derived for obtaining the optimal trajectories. In the following development, the C_F - C_L diagram is presented and discussed, and the solution procedure is derived.

Equations (21) and (22) can be used, for a given airplane-engine configuration, to construct a C_F - C_L diagram of all possible optimal interior arcs. The airplane-engine data used here are representative of a supersonic transport (SST). The assumed values of the airplane parameters are given in table I, along with the inverse atmospheric scale height β.

The specific fuel consumption S is shown as a function of C_F in figure 2. The value of S is constant until afterburning is initiated at C_F^*, after which S increases with C_F. The data in table I and figure 2 apply at a velocity of 754.3 meters per second (corresponding to a Mach number of 2.7).

From equations (21) and (22), define

$$f(C_F) = C_F - C_{D,0} - \frac{a}{a'} \tag{26a}$$

$$b(C_F) = C_F - C_{D,0} - \frac{a}{\beta v} \tag{26b}$$

Then equations (21) and (22) become

$$\dot{C}_F = \frac{a'}{a''C_L}\left(\beta v - a'\right)\left(f + KC_L^2\right) \tag{27a}$$

$$\dot{C}_L = \beta v\left(b - KC_L^2\right) \tag{27b}$$

Also,

$$f' = \frac{aa''}{(a')^2} \tag{28a}$$

$$b' = 1 - \frac{a'}{\beta v} \tag{28b}$$

Since $a'' \geq 0$ and $a' < \beta v$ for the values assumed, f and b are monotonically increasing functions of C_F (see eqs. (28)). Also, $f(C_F)$ is negative for all values of C_F, while $b(C_{F,l})$ is negative and $b(C_{F,u})$ is positive. These characteristics define the shape of the $\dot{C}_F = 0$ and $\dot{C}_L = 0$ curves, as shown in figure 3. Above the $\dot{C}_F = 0$

10

curve, C_F increases; below, C_F decreases. Above the $\dot{C}_L = 0$ curve, C_L decreases; below, C_L increases. The intersection of the $\dot{C}_F = 0$ and $\dot{C}_L = 0$ curves is the modified-Breguet-cruise (MBC) point, as discussed previously in connection with equations (24) and (25). For each C_F, C_L combination, the values of $\dot{C}_F$ and $\dot{C}_L$ are uniquely determined (although not shown explicitly). Thus, for a given C_F, C_L starting point, the entire optimal trajectory is determined from that point on.

In figure 3, a discontinuity in C_F exists between C_F^* and $C_{F,\,l}$. This discontinuity is due to the constant S assumed for values of C_F less than C_F^*, which results in $a'' = 0$ for these values and makes $\dot{C}_F$ increase to infinity in equation (27a). Thus, when C_F decreases to C_F^* on an interior arc, it will jump to $C_{F,\,l}$. Alternatively, trajectories starting at $C_{F,\,l}$ will jump to C_F^* if an interior arc is required.

Four regions are defined in figure 3 by the $\dot{C}_F = 0$ and $\dot{C}_L = 0$ curves and their intersection. In region I, C_F decreases and C_L increases; in region II, C_F and C_L both decrease; in region III, C_F increases and C_L decreases; and in region IV, C_F and C_L both increase. The following optimal trajectories are illustrated in the figure:

(1) Trajectory A starts in region I. First C_F decreases while C_L increases to the $\dot{C}_L = 0$ curve. Then C_L decreases and C_F decreases to C_F^*; C_F then jumps to $C_{F,\,l}$ and C_L decreases.

(2) Trajectory B starts in region I. First C_L increases while C_F decreases to $\dot{C}_F = 0$. Then C_L increases while C_F increases to $C_{F,u}$. Finally, C_L increases while C_F remains at $C_{F,u}$.

(3) Trajectory C starts in region III. As C_L decreases, C_F increases to $\dot{C}_F = 0$. Then C_L decreases while C_F decreases to $C_{F,\,l}$ and remains at that value.

(4) Trajectory D starts in region III. As C_F increases, C_L decreases to the $\dot{C}_L = 0$ curve. Then C_L increases and C_F increases to $C_{F,u}$. Finally, C_L increases while C_F remains at $C_{F,u}$.

For all trajectories starting in region II, C_L decreases and C_F decreases to C_F^*, while in region IV, C_L increases and C_F increases to $C_{F,u}$.

An additional question that remains is the number of interior arcs which can occur for a single optimal trajectory. A related question is whether the value of C_F can jump discontinuously from $C_{F,\,l}$ to $C_{F,u}$ or vice versa, or if interior arcs must be used for this transition.

The former question can be answered by referring to figure 3. From this figure it can be seen that all interior arcs which terminate at $C_{F,u}$ arrive at $C_{F,u}$ in region IV. In this region, $\dot{C}_L$ is positive, so that the trajectory can never return to region I (along the line $C_F = C_{F,u}$) to start another interior arc. Similar reasoning shows that once C_F has reached $C_{F,\,l}$ (regions I or II), it can never return to region III to start another interior arc.

Additional interior arcs might still exist if C_F could jump discontinuously from $C_{F,l}$ to $C_{F,u}$ or vice versa. Then, for example, C_F could jump from $C_{F,l}$ to $C_{F,u}$ while $C_L = 0.01$, and a second interior arc could start at that point. To show that this is not possible, consider first equation (16). The control C_F is chosen to minimize H, and if λ_2 is positive, H can always be made negative by choosing C_F such that the coefficient of λ_1 has the same sign as λ_1. However, H = 0 for a free-time optimum solution. Therefore, λ_2 must be negative. Now if C_F can jump from $C_{F,u}$ to $C_{F,l}$, $H(C_{F,u}) = H(C_{F,l})$ at the transition time. But from equation (19),

$$\frac{\partial^2 H}{\partial C_F^2} = - \frac{\lambda_2 A Q a''}{g} + 2\mu \geq 0$$

so that $H(C_F)$ is convex. Therefore, if $H(C_{F,u}) = H(C_{F,l})$, $H(C_F) < H(C_{F,u})$ for every intermediate value of C_F, as shown in sketch (a).

(a)
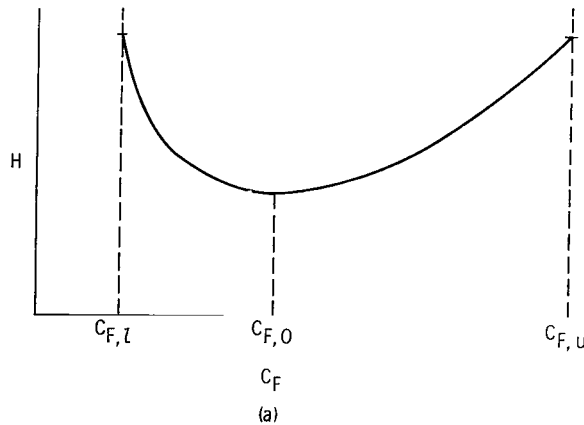
Hence, C_F would be equal to $C_{F,0}$, and not $C_{F,u}$ or $C_{F,l}$. Therefore, no jumps from $C_{F,u}$ to $C_{F,l}$ (or vice versa) are possible. Furthermore, the convexity of $H(C_F)$ verifies the optimality of interior arcs, since it demonstrates that the necessary condition in equation (19) is satisfied for such arcs.

The previous discussion proves that the control history for an optimal trajectory consists (at most) of one maximum, one minimum, and one interior arc. Furthermore, the optimal trajectory is unique.

RESULTS AND DISCUSSION

Long-Duration Cruise

As noted earlier, the values of C_F and C_L do not change with time at the MBC point. Although not shown explicitly in figure 3, the values of C_L and C_F change slowly with time near the MBC point, but change quite rapidly away from this point. For example, trajectory A in figure 3 requires 6.25 minutes and has a range of 283 kilometers. The initial and final altitudes are both 9.15 kilometers. Trajectory B requires only 1.54 minutes to climb from 9.15 kilometers to $C_{F,u}$ at an 18.29-kilometer altitude. The range traversed is 69.4 kilometers. Trajectory C starts at 21.37 kilometers and requires 8.42 minutes to descend to 9.15 kilometers, while covering a range of 381.4 kilometers.

While these trajectories are optimal, they are not normally of interest since an SST must cruise for long periods of time (several hours). Since trajectories A to C have durations of several minutes, it is clear that optimal cruise trajectories of several hours duration must spend much time very near the MBC point. In fact, it is reasonable to assume that such trajectories include a long-duration phase at the MBC point, together with connecting arcs to the initial and final conditions.

Figure 3 may be used to determine how such trajectories can be numerically constructed. A comparison of trajectories A and B in region I indicates that there is a unique trajectory, between A and B, which terminates at the MBC point. All other trajectories in region I diverge from this point. Similarly, a single trajectory exists in region III which terminates at the MBC point, which lies between trajectories C and D. Also, there are only two trajectories which leave the MBC point, and these lie in regions II and IV. The four trajectories of this type are shown in figure 4. The optimal trajectories then start with connecting arc 1 or 3 (depending on the initial altitude), continue with an MBC, and conclude with connecting arc 2 or 4, again depending on the desired final altitude. Since trajectories generally consist of climb, cruise, and descent, connecting arcs 1 and 2 will normally be used. Connecting arc 1 is the climb-transition arc between the starting point and the MBC point, while connecting arc 2 is the descent-transition arc. These transition arcs correspond to those phases of the trajectory in which the airplane is at cruise velocity but not at optimum altitude for the MBC.

It has been established that the long-duration cruise trajectories of interest consist essentially of two definite connecting arcs (with end points depending on the initial and final values of mass and altitude) and an MBC. It remains to determine the values of C_L, C_F, and m, as functions of time, on connecting arcs 1 and 2. For connecting arc 1, these values are best determined by numerical integration backwards in time from the MBC point. For connecting arc 2, the integration is performed forward from the

MBC point. In both cases, the initial values of C_L and C_F are perturbed a small amount from the MBC values into the proper region. This procedure gives small, but nonzero, values of $\dot{C}_L$ and $\dot{C}_F$ which are needed to start the integration of equations (21) and (22).

The resulting values are presented in figures 5 to 10. The initial value of C_L, $C_{L,0}$, is shown as a function of time spent on connecting arc 1 in figure 5. The required value of $C_{L,0}$ is a function of the initial altitude and mass. For convenience, C_L/m is plotted as a function of initial altitude in figure 6. From this figure, $C_{L,0}$ can be easily determined. The ratio of the mass at the start of the MBC to the initial mass m_{SBC}/m_0 is also a function of connecting arc time t_{SBC}. This may be seen by rewriting equation (15b) as

$$\dot{m} = \frac{-AQ}{g} C_F S = -\frac{ma}{C_L}$$

Since C_F and C_L are definite functions of time, this equation may be integrated to give

$$\frac{m_0}{m_{SBC}} = \exp\left[\int_0^{t_{SBC}} \frac{a(C_F)}{C_L} dt\right]$$

The result is shown in figure 7. Thus, connecting arc 1 is completely determined for given values of initial mass and altitude from figures 5 and 7. Similar data are presented for connecting arc 2 in figures 8 and 9. Figure 8 shows $C_{L,f}$ as a function of time spent on connecting arc 2, while figure 9 gives the mass ratio m_{EBC}/m_f.

For given values of initial and final mass and altitude, the time spent on connecting arcs 1 and 2 is determined, as are the initial and final mass at the MBC point. It remains to calculate the time spent on the MBC arc t_{BC}. This time may be calculated by integrating equation (15b), which results in

$$t_{BC} = \left(\frac{C_L}{C_F S}\right)_{BC} \log\left(\frac{m_{SBC}}{m_{EBC}}\right) \tag{29}$$

where the values of C_L, C_F, and S are those of the MBC arc. The results of equation (29) are plotted in figure 10 for convenience. However, for greater accuracy, equa-

tion (29) should be used in calculating t_{BC}. For the parameters assumed in this report, $(C_L/C_F S)_{BC} = 4.8972$ hours.

In order to illustrate the use of the figures, an example is given. Suppose

$$m_0 = 291\,000 \text{ kg}$$

$$m_f = 184\,000 \text{ kg}$$

$$h_0 = h_f = 9.2 \text{ km}$$

Then from figure 6,

$$\frac{C_L}{m} = 1.0 \times 10^{-7} \text{ kg}^{-1}$$

$$C_{L,0} = 1.0 \times 10^{-7}\, m_0 \approx 0.0291$$

$$C_{L,f} = 1.0 \times 10^{-7}\, m_f = 0.0184$$

Next, from figure 5,

$$t_{SBC} = 10.35 \text{ min}$$

and from figure 7,

$$m_{SBC} = 0.9585\, m_0 = 278\,924 \text{ kg}$$

From figure 8,

$$t_{EBC} = 12.9 \text{ min} \quad \textit{for } C_{L,f} = .0184$$

and from figure 9,

$$m_{EBC} = 1.0502\, m_f = 193\,237 \text{ kg}$$

Now from equation (28), for $m_{EBC}/m_{SBC} = 0.692795$,

$$t_{BC} = 1.7974 \text{ hr}$$

Therefore, the total trip time is

$$t = 10.35 + 60(1.7974) + 12.9 = 131.1 \text{ min}$$

and the total cruise range is

$$R = Vt = 5934 \text{ km}$$

It is interesting to compare the maximum range with the corresponding range which would be obtained if the standard procedure is used to generate the connecting arcs. With the standard procedure, the maximum thrust coefficient is used to climb to the Breguet cruise altitude, and minimum C_F is used to descend from the Breguet cruise altitude to the final altitude. A comparison of standard trajectory range is made with the optimal range in figure 11, for $m_0 = 291\,200$ kilograms and $m_f = 184\,200$ kilograms. The range increase obtained by using the optimal trajectories is plotted as a function of initial altitude. The initial and final altitudes are assumed to be the same. The results in figure 11 show that the range improvement is small, less than 7 kilometers even for initial and final altitudes as low as 9 kilometers (the optimal initial MBC altitude is about 17.4 km).

Short-Duration Cruise

It is reasonable to expect that the range difference will always be small whenever the flight is of long enough duration so that it is advantageous to reach the Breguet cruise altitude. However, for very short duration flight starting from a relatively low altitude, the entire optimal trajectory is a connecting arc which remains below the Breguet cruise altitude, and the range penalty incurred by using the standard trajectory could be important.

Therefore, a comparison of optimal trajectory range with standard trajectory range was made for propellant masses ranging from 0 to 17 000 kilograms. The results are presented in figure 12, for initial and final altitudes of 9.15 kilometers and a final mass of 184 200 kilograms. For fuel mass up to 6900 kilograms, the standard trajectory consists only of maximum and minimum thrust arcs, since there is insufficient fuel for the standard trajectory to reach the Breguet cruise altitude. The range increment increases

to a maximum of about 9 kilometers at a fuel mass of 6900 kilograms. For fuel masses greater than this value, the standard trajectory also includes a Breguet cruise segment of the required duration. The range increment then decreases rapidly to about 7 kilometers. The optimum trajectory consists of an interior arc for fuel masses up to 17 000 kilograms. At this point, the connecting arc passes so close to the MBC point that a Breguet cruise phase is included.

For short-range (low-propellant-mass) cruise, a constant-altitude trajectory might reasonably be considered to be a good approximation to the optimum. A comparison of optimum cruise range with constant-altitude cruise range is presented in figure 13 as a function of fuel mass. As in figure 12, the initial and final altitudes are 9.15 kilometers, and the final mass is 184 200 kilograms. It can be seen from the figure that constant-altitude cruise is a poor approximation to the optimum even for small fuel masses. For example, the range increment is 510 kilometers for a fuel mass of 15 000 kilograms.

VERIFICATION OF APPROXIMATIONS

In the derivation of the optimal trajectories presented, it was assumed that γ is small and that the normal acceleration is negligible. These approximations may be checked at this point by observing the resulting values on the optimal trajectories.

The value of γ may be determined by setting $\dot{v}$ (eq. (12a)) equal to zero, which results in

$$\sin \gamma = \frac{QA}{mg} (C_F - C_D)$$

For long-duration cruise, the largest values of γ occur on the climb-transition arc. The value of γ on this arc is shown as a function of time in figure 14 for a trajectory starting at an 11.4-kilometer altitude. The altitude profile is also presented in this figure. For values of γ less than 8°, $\cos \gamma$ is greater than 0.99, so that the approximation $\cos \gamma = 1$ is valid to within 1 percent. Figure 14 shows that γ is less than 8° for altitudes greater than about 13.4 kilometers. Furthermore, even if the initial altitude is as low as 9 kilometers, the time required to ascend to 13 kilometers is less than 1/2 minute (out of a total trajectory time of several hours). Therefore, the small angle approximation seems to be valid.

Consider next the approximation of neglecting normal acceleration. In equation (12b), $\dot{\gamma}$ was neglected and C_L was set equal to mg/QA. The effect of the approximation is to

neglect the lift required to change γ. The true required lift coefficient is given by

$$C_L^* = C_L\left(\cos \gamma + \frac{v\dot{\gamma}}{g}\right)$$

where

$$C_L = \frac{mg}{QA}$$

is the approximate lift coefficient. The approximate and true lift coefficients are plotted in figure 15 as a function of time on the climb-transition arc. The difference between C_L and C_L^* is small near the MBC altitude, but increases to 0.03 at an altitude of 11.4 kilometers. The error in lift coefficient results in an error in drag coefficient (C_D is a function of C_L), which changes C_F by an equal amount in order to maintain the desired climb rate. The true drag coefficient is given by

$$C_D^* = C_{D,0} + K(C_L^*)^2$$

and is plotted in figure 16 along with the approximate drag coefficient as a function of time on the climb-transition arc. Figure 16 shows that the error in C_D (hence C_F) is fairly small (less than 10 percent for altitudes above 13 km) even though the error in C_L is large. Furthermore, the amount of time spent in the low-altitude region, where the error is substantial, is very short relative to the total cruise time. Therefore, neglecting normal acceleration represents a reasonable approximation.

CONCLUDING REMARKS

The problem of maximizing range for constant-velocity flight between fixed terminal conditions (mass and altitude) has been studied. Normal acceleration is neglected, as in the derivation of the Breguet cruise, but the thrust required to change altitude is included. Range is maximized for a supersonic airplane and compared to the range obtained by using the standard trajectory, consisting of a Breguet cruise arc and maximum- and minimum-thrust connecting arcs. The difference between optimum and standard trajectory range was shown to be small. However, the optimal range can be calculated without

great difficulty, as described in this report. Therefore, the method derived in this report should be considered for use in cruise trajectory calculations.

Lewis Research Center,
    National Aeronautics and Space Administration,
        Cleveland, Ohio, December 13, 1971,
            110-06.

APPENDIX - SYMBOLS

A reference area, m^2

a, b functions of C_F introduced for notational simplicity

C_D drag coefficient, nondimensional

C_D^* true drag coefficient, nondimensional

$C_{D,0}$ zero-lift drag coefficient, nondimensional

C_F thrust coefficient, nondimensional

C_F^* minimum C_F for afterburning, nondimensional

C_L lift coefficient, nondimensional

C_L^* true lift coefficient, nondimensional

D drag, N

f function of C_F introduced for notational simplicity

g acceleration due to gravity, m/sec^2

H variational Hamiltonian, m/sec

h altitude, m

K slope of drag polar, nondimensional

L lift, N

m mass, kg

Q dynamic pressure, N/m^2

R range, km

S specific fuel consumption, sec^{-1}

T thrust, N

t time, sec

v velocity, m/sec

β exponent for isothermal atmosphere, m^{-1}

γ flight path angle, rad or deg

λ_1 costate variable, $(m^2)(sec^2)/kg$

λ_2 costate variable, m/kg

μ costate variable, m/sec

ρ density, kg/m^3

ρ_0 surface density, kg/m^3

Subscripts:

BC   Breguet cruise

EBC   end Breguet cruise

f   final

l lower limit

u   upper limit

SBC   start Breguet cruise

0   initial

Superscripts:

·   derivative with respect to time

•   derivative with respect to thrust coefficient

REFERENCES

1. Bryson, Arthur E., Jr.; Desai, Mukund N.; and Hoffman, William C.: Energy-State Approximation in Performance Optimization of Supersonic Aircraft. J. Aircraft, vol. 6, no. 6, Nov.-Dec. 1969, pp. 481-488.

2. Denham, Walter F.: Steepest-Ascent Solution of Optimal Programming Problems. Ph.D. Thesis, Harvard University, 1963.

3. Pontryagin, L. S.; Boltyanskii, V. G.; Gamkrelidze, R. V.; and Mischenko, E. F. (K. N. Trirogoff, trans.): The Mathematical Theory of Optimal Processes. Interscience Publishers, 1962.

TABLE I. - AIRPLANE AND ATMOSPHERIC CONSTANTS

Velocity, v, km/sec 0.7543

Reference area, A, m^2 704

Slope of drag polar, K 0.5

Zero-lift drag coefficient, $C_{D,0}$ 0.00878

Exponent for isothermal atmosphere, β, km^{-1} 0.16
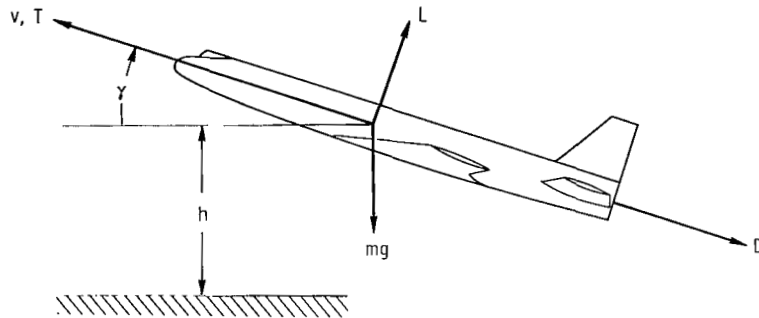
Figure 1. - Definition of trajectory variables.
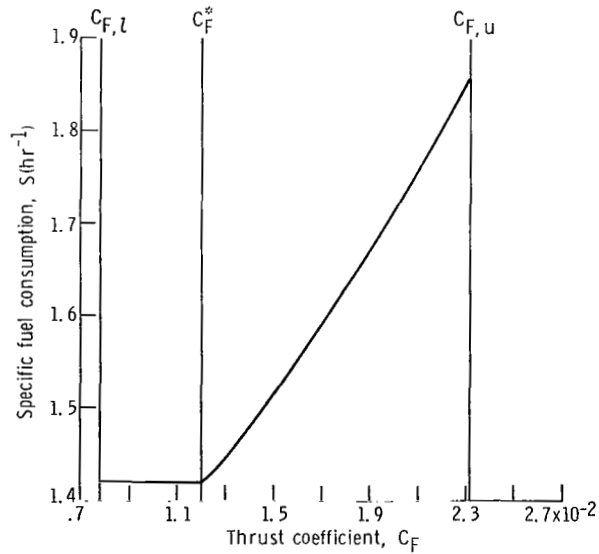
Figure 2. - Specific fuel consumption as function of thrust coefficient.

23
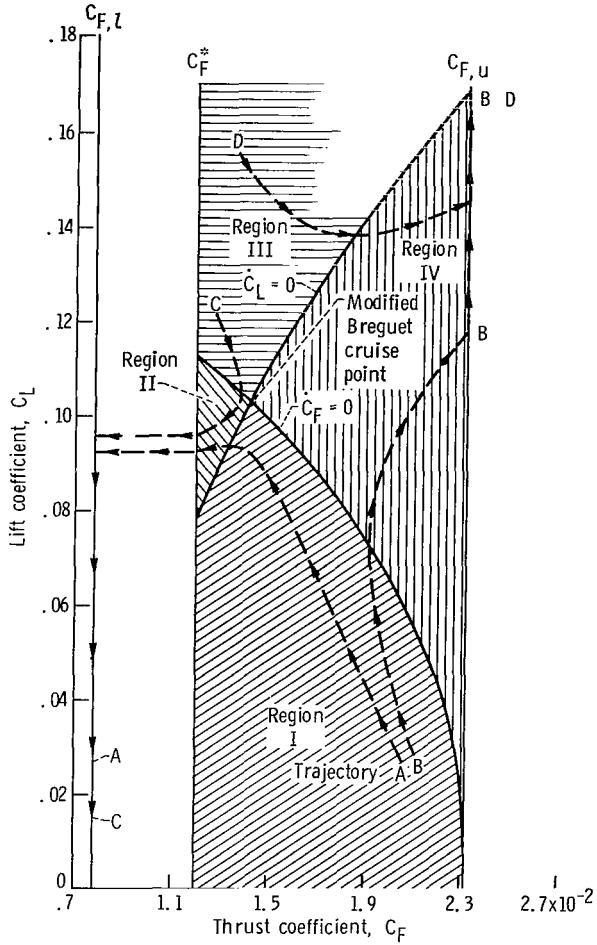
Figure 3. - Lift coefficient as function of thrust coeffi-
cient. Four possible optimal trajectories and modified
Breguet cruise point illustrated.
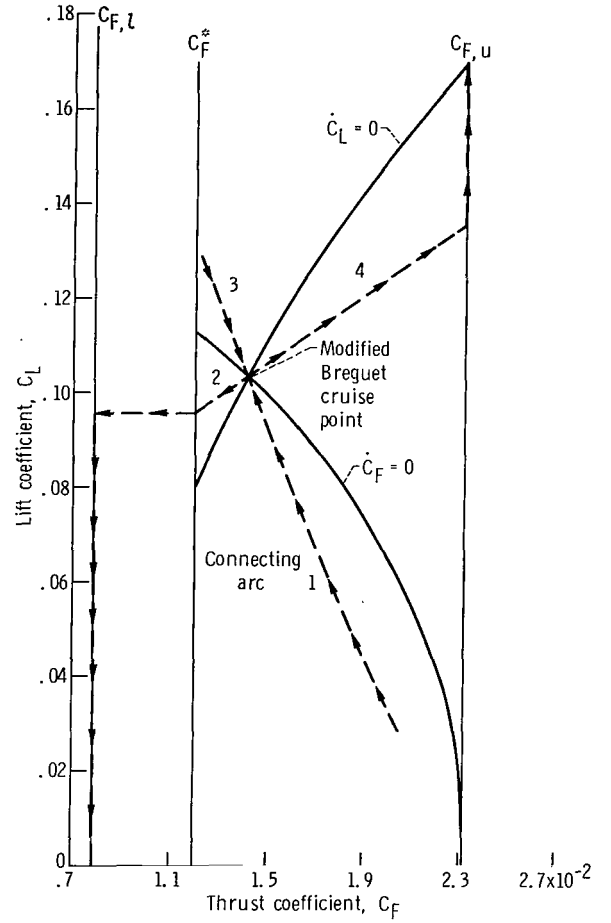
Figure 4. - Lift coefficient as function of thrust coeffi-
cient. Connecting arcs to and from modified Breguet
cruise point illustrated.
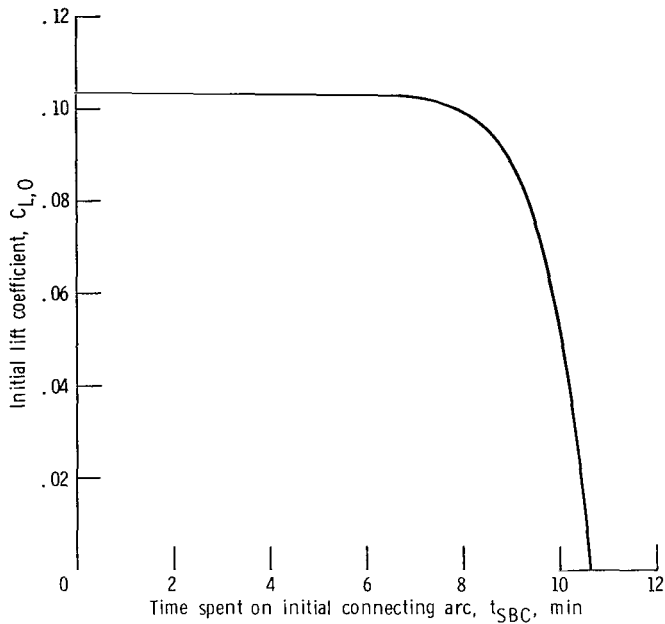
Figure 5. – Initial value of lift coefficient.
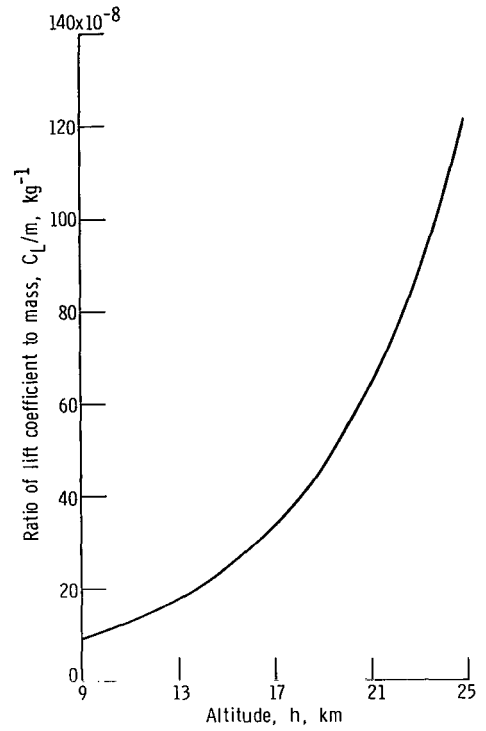
Figure 6. – Ratio of lift coefficient to mass.
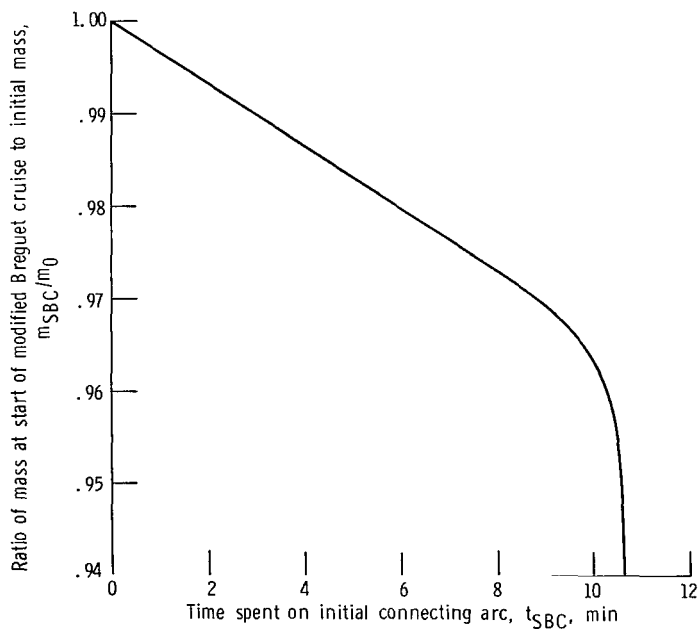
Figure 7. – Ratio of mass at start of Breguet cruise to initial mass.
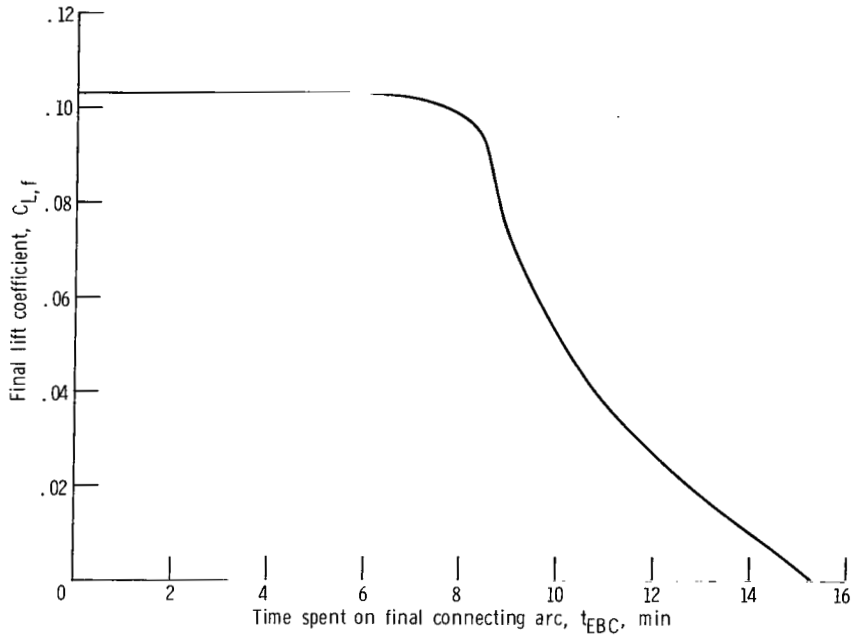
Figure 8. – Final value of lift coefficient.
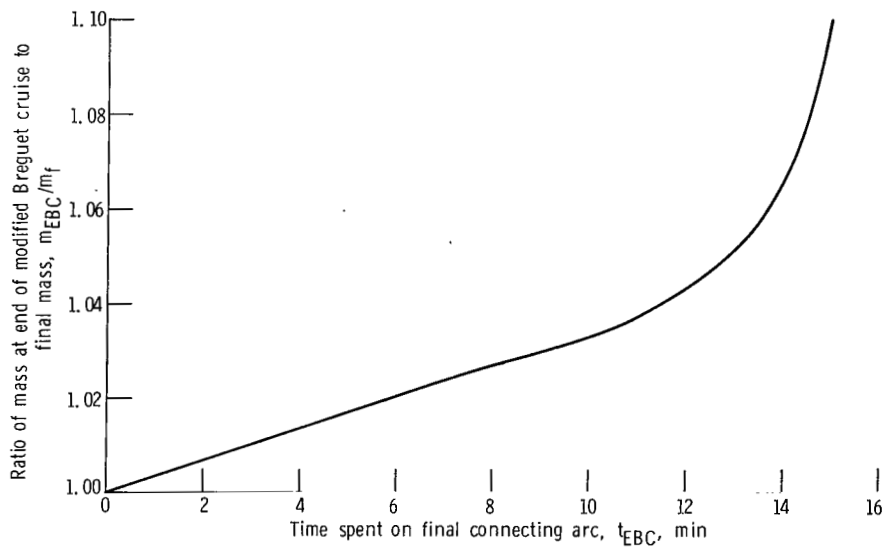
Figure 9. – Ratio of mass at end of modified Breguet cruise to final mass.
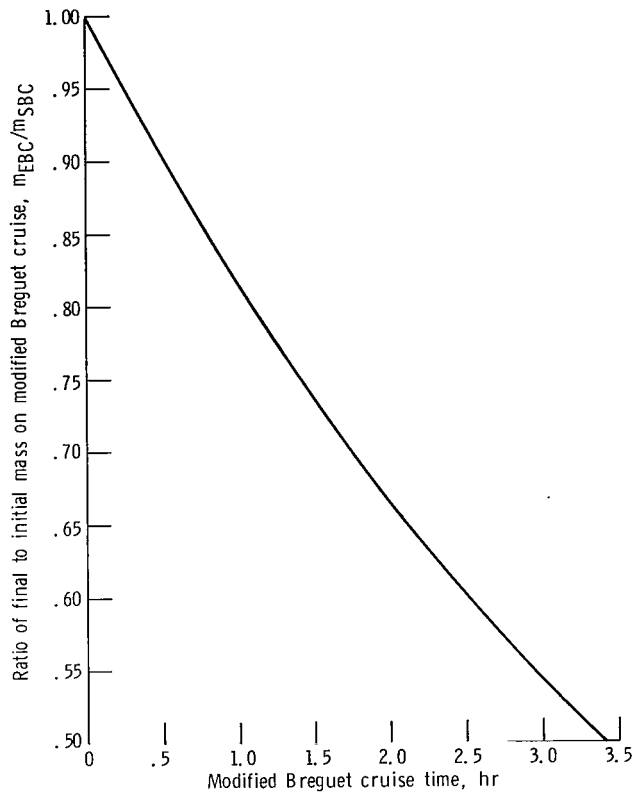
Figure 10. - Ratio of final to initial mass on modified Breguet cruise.
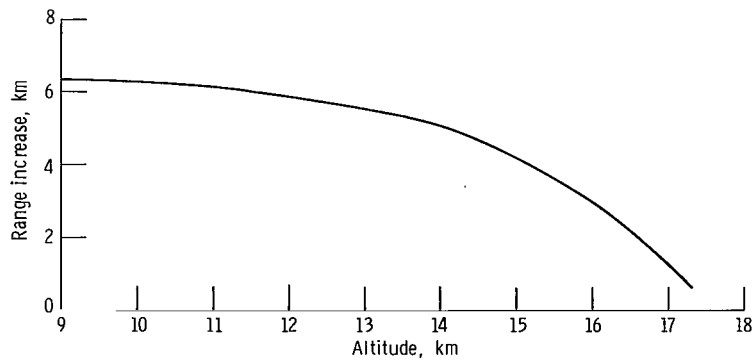
Figure 11. - Range increase of optimal trajectory over standard trajectory as function of initial altitude for long-duration flights. Initial mass, 291 200 kilograms; fuel mass, 107 000 kilograms.
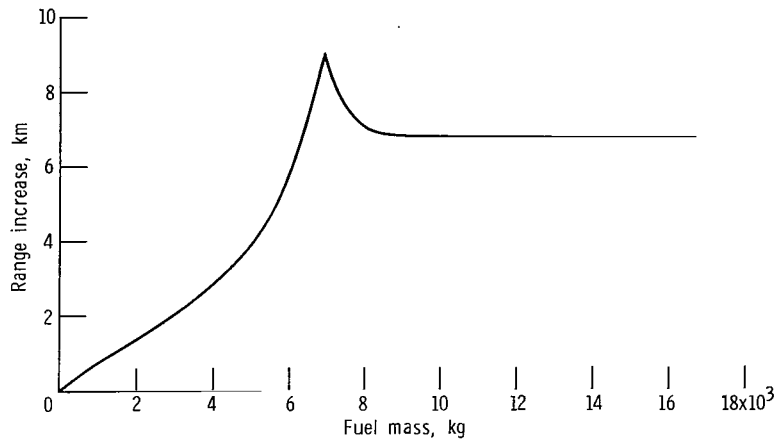
Figure 12. - Range increase for short-duration flight of optimal trajectory over standard trajectory as function of fuel mass. Final mass, 184 200 kilograms; initial and final altitudes, 9.15 kilometers.
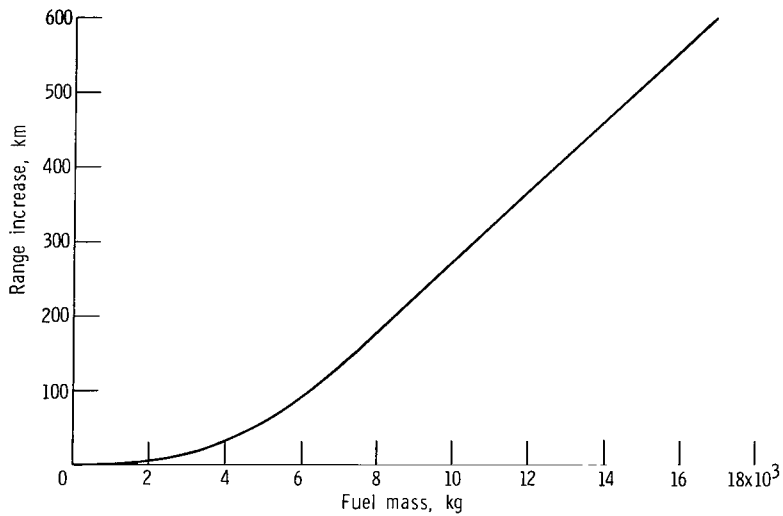
Figure 13. - Range increase for short-duration flight of optimal trajectory over constant-altitude (9.15-km) trajectory as function of fuel mass.

28
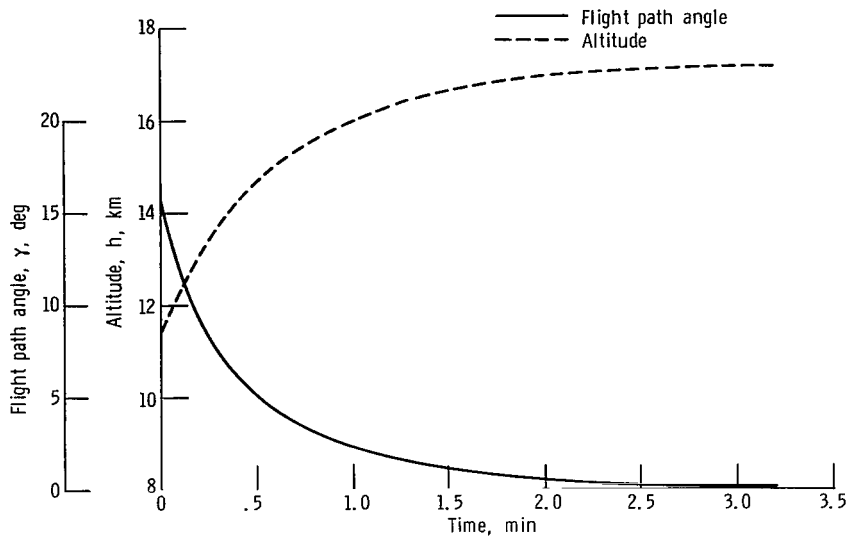
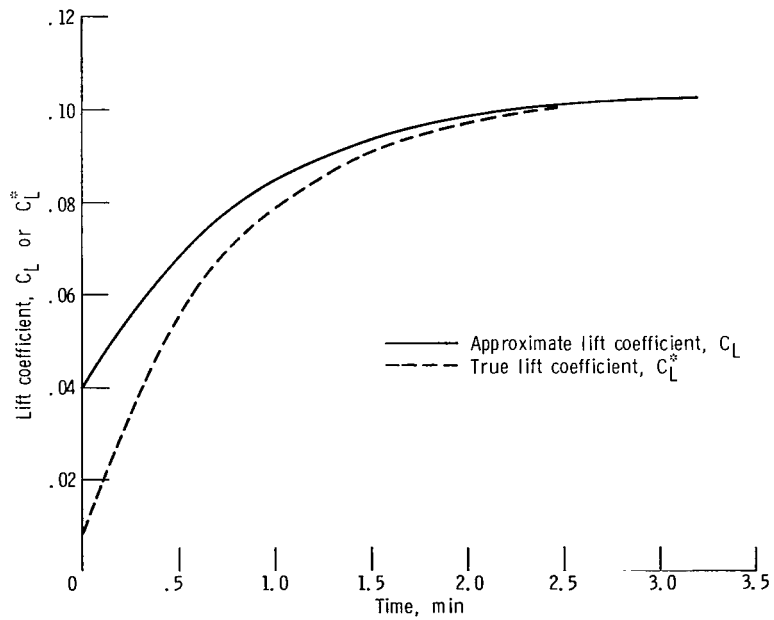Figure 14. - Trajectory variables on climb-transition arc.

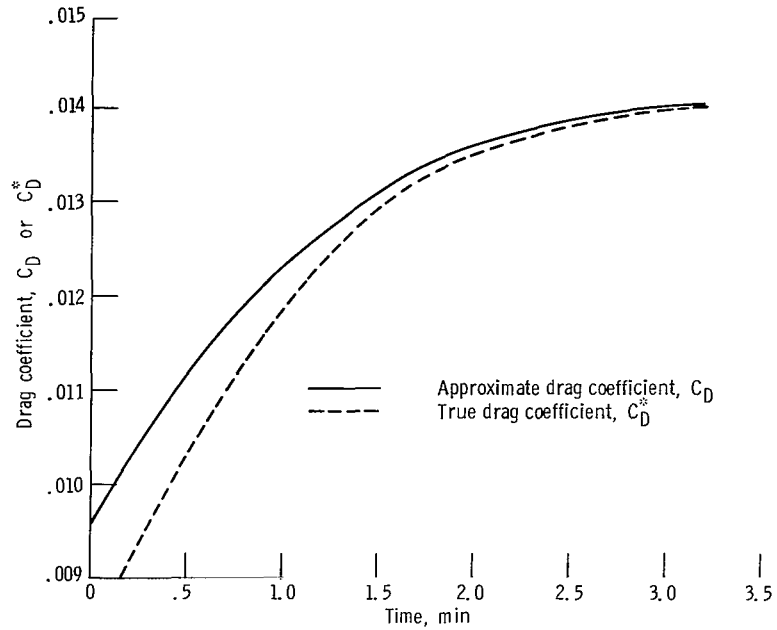Figure 15. - Approximate and true lift coefficients on climb-transition arc.

29

Figure 16. - Approximate and true drag coefficients on climb-transition arc.

"The aeronautical and space activities of the United States shall be conducted so as to contribute . . . to the expansion of human knowledge of phenomena in the atmosphere and space. The Administration shall provide for the widest practicable and appropriate dissemination of information concerning its activities and the results thereof."

— NATIONAL AERONAUTICS AND SPACE ACT OF 1958

NASA SCIENTIFIC AND TECHNICAL PUBLICATIONS

TECHNICAL REPORTS: Scientific and technical information considered important, complete, and a lasting contribution to existing knowledge.

TECHNICAL NOTES: Information less broad in scope but nevertheless of importance as a contribution to existing knowledge.

TECHNICAL MEMORANDUMS: Information receiving limited distribution because of preliminary data, security classification, or other reasons.

CONTRACTOR REPORTS: Scientific and technical information generated under a NASA contract or grant and considered an important contribution to existing knowledge.

TECHNICAL TRANSLATIONS: Information published in a foreign language considered to merit NASA distribution in English.

SPECIAL PUBLICATIONS: Information derived from or of value to NASA activities. Publications include conference proceedings, monographs, data compilations, handbooks, sourcebooks, and special bibliographies.

TECHNOLOGY UTILIZATION PUBLICATIONS: Information on technology used by NASA that may be of particular interest in commercial and other non-aerospace applications. Publications include Tech Briefs, Technology Utilization Reports and Technology Surveys.

Details on the availability of these publications may be obtained from:

SCIENTIFIC AND TECHNICAL INFORMATION OFFICE

NATIONAL AERONAUTICS AND SPACE ADMINISTRATION

Washington, D.C. 20546